

Neutral current four-fermion production in e^+e^- collisions at $\sqrt{s} = 130-183$ GeV.

Preliminary

DELPHI Collaboration

P. Bambade¹, M. Barbi², M. Begalli², G. Borissov¹, H. Carvalho³,
K. Cieslik⁴, R. Contri⁵, D. Crennell⁶, J. Cuevas⁷, S. Gamblin¹, J. Heuser⁸,
R. Keranen⁹, N. Kjaer¹⁰, J. R. Mahon², J. Marco¹¹, L. Mundim²,
J. Palacios¹², H. Palka¹³, C. Parkes¹⁴, H. T. Phillips⁶, M. E. Pol³,
P. Renton¹², I. van Vulpen¹⁰, M. Witek⁴.

Abstract

We present preliminary results on data accumulated by the DELPHI detector at centre-of-mass energies ranging from 130 GeV to 183 GeV. The observed numbers of events containing four final-state fermions produced primarily by neutral current processes such as ZZ and $Z\gamma^*$ (states produced primarily via W^+W^- production are reported elsewhere) are compared with Standard Model predictions.

Paper submitted to the ICHEP'98 Conference
Vancouver, July 22-29

¹ LAL, Orsay

² UERJ, Rio de Janeiro

³ CBPF, Rio de Janeiro

⁴ Institute of Nuclear Physics, Cracow

⁵ INFN/Univ. Genova, Genova

⁶ Rutherford Appleton Laboratory, Chilton

⁷ Universidad de Oviedo, Oviedo

⁸ Gesamthochschule Wuppertal Bergische, Wuppertal

⁹ Institut. für Exper. Kernphysik, Karlsruhe

¹⁰ NIKHEF, Amsterdam

¹¹ Instituto de Fisica de Cantabria, CSIC, Spain

¹² Nuclear Physics Laboratory, Oxford

¹³ Institute of Nuclear Physics, Cracow. This work supported in part by KBN Grant 2P03B03311

¹⁴ CERN, Geneva



1 Introduction

Four-fermion processes become increasingly important in e^+e^- interactions as the centre-of-mass energy increases. LEP2 is now operating in an energy regime where on-shell ZZ production is predicted. In this paper a search is made for this as well as for other four-fermion processes. Such processes also form an important background to new particle searches at LEP2 and a deviation from the Standard Model expectation would be a signal of new physics.

At 130-140 GeV the four-fermion production cross section is dominated by neutral current processes. At higher energies (above the W pair threshold at 161 GeV), W^+W^- production becomes dominant. We have reported on the measurement of cross-sections for this processes elsewhere [1][2]. This study updates and extends our earlier study [3] of the neutral current dominated processes $l^+l^-q\bar{q}$ and $l^+l^-l^+l^-$. We also present measurements of the cross-sections for producing $q\bar{q}q\bar{q}$ at 183 GeV in the region of phase space where on-shell ZZ production contributes. For the purposes of this discussion we define the on-shell ZZ region as the region where the masses of both pairs of final-state fermions is within 20 GeV/ c^2 of the nominal Z mass, taken to be 91.1888 GeV/ c^2 .

2 Detector description

A summary of the properties of the DELPHI detector relevant to this analysis is presented below. A more detailed description can be found in [4].

Charged particle tracks were measured in a system of cylindrical tracking chambers immersed in a 1.2 T solenoidal magnetic field. These were the Microvertex Detector (VD), the Inner Detector (ID), the Time Projection Chamber (TPC), and the Outer Detector (OD). In addition, two planes of drift chambers aligned perpendicular to the beam axis (Forward Chambers A and B) tracked particles in the forward and backward directions, covering polar angles $11^\circ < \theta < 33^\circ$ and $147^\circ < \theta < 169^\circ$.

The electromagnetic calorimetry consisted of the High density Projection Chamber (HPC) covering the barrel region of $40^\circ < \theta < 140^\circ$, the Forward ElectroMagnetic Calorimeter (FEMC) covering $11^\circ < \theta < 36^\circ$ and $144^\circ < \theta < 169^\circ$ and the STIC, a scintillator tile calorimeter which extends the coverage down to 1.66° in the forward and backward regions. The 40° taggers were a series of single-layer lead-scintillator counters used to veto electromagnetic particles otherwise missed in a region between HPC and FEMC. The hadron calorimeter (HCAL) covered 98% of the solid angle. Muons with momenta above 2 GeV can pass through the HCAL; these were recorded in a set of Muon Drift Chambers.

3 Data samples

The integrated luminosities accumulated by DELPHI at energies above the Z^0 peak during 1995, 1996 and 1997 are shown in table 1.

Simulated events were produced with the DELPHI simulation program DELSIM[5] and were then passed through the same reconstruction chain as the data. Processes leading to four-fermion final states were generated with EXCALIBUR[6], relying on JETSET 7.4 [7] for quark fragmentation. EXCALIBUR includes all tree-level diagrams in a consistent fashion.

Year	Centre-of-Mass Energy (GeV)	Integrated Luminosity (pb^{-1})
1995	130.4	2.9
1995	136.2	3.0
1995	140.0	0.1
1996	161.0	9.9
1996	172.0	10.0
1997	130.4	3.0
1997	136.2	2.9
1997	182.7	54.0

Table 1: Integrated luminosity collected by DELPHI at each centre-of-mass energy during high-energy LEP runs in 1995 to 1997. (No run quality criteria were applied.)

Initial state radiation was treated using the QEDPS program[8] for those final states which did not include e^+e^- pairs; for final states including e^+e^- the default EXCALIBUR collinear treatment was used.

Cuts were imposed at generator level on the invariant mass of fermion-antifermion pairs and on $\cos\theta_e$, the cosine of the angle of electrons relative to the electron beam and positrons relative to the positron beam. This was necessary because EXCALIBUR treats all fermions as having zero mass and hence the cross-sections diverge unless suitable cuts are applied. The requirements used at 183 GeV are shown in table 2.

The background processes $e^+e^- \rightarrow f\bar{f}(n\gamma)$ were generated using PYTHIA [7]. PYTHIA was also used to generate four-fermion final states via the processes $(Z^0/\gamma)^*(Z^0/\gamma)^*$, W^+W^- , $W e\nu_e$ and $Z^0 e^+e^-$ which were used to cross-check EXCALIBUR. PYTHIA does not include all tree-level diagrams so the above processes must be added incoherently. However, it does have an approximate treatment of the transverse momentum of initial state radiation photons for all final states. Two-photon interactions were generated using TWOGAM [9] and BDK [10].

Quantity	Requirement
$\cos\theta_e$	< 0.98 in $e^+e^-l^+l^-$
$\cos\theta_e$	< 0.9999 otherwise
$M(e^+e^-)$	> 0.05 GeV/ c^2 in $e^+e^-l^+l^-$
$M(e^+e^-)$	> 1.0 GeV/ c^2 otherwise
$M(\mu^+\mu^-)$	> 0.21 GeV/ c^2
$M(\tau^+\tau^-)$	> 3.6 GeV/ c^2
$M(d\bar{d})$	> 2 GeV/ c^2
$M(u\bar{u})$	> 2 GeV/ c^2
$M(s\bar{s})$	> 2 GeV/ c^2
$M(c\bar{c})$	> 5 GeV/ c^2
$M(b\bar{b})$	> 15 GeV/ c^2

Table 2: Requirements made at generator level on electron/positron angles and masses of fermion-antifermion pairs for the EXCALIBUR samples used in the analysis at 183 GeV.

4 Jets and a pair of isolated leptons

The two final state leptons in the process $e^+e^- \rightarrow l^+l^-q\bar{q}$ are typically well isolated from all other particles. This property can be used to select such events with high efficiency in both the muon and electron channels¹. Events were selected initially without explicit cuts on the masses of the final state fermion pairs in order to select both ZZ and $Z\gamma^*$ events; mass cuts were then applied to isolate the on-shell ZZ component.

¹Events with $\tau^+\tau^-$ pairs are not considered here.

4.1 $\mu^+\mu^-q\bar{q}$ final states

Muons were identified using the standard DELPHI algorithm [4]. Events were required to have at least 6 charged particles and a charged energy above $0.30\sqrt{s}$. A particle was considered isolated if its momentum was larger than $5\text{ GeV}/c$ and if the total momentum of all charged particles present within a 5° cone around its direction did not exceed 15% of its momentum and was less than $5\text{ GeV}/c$. At least two such particles with opposite charge were required and at least one of them was required to be identified as a muon for the event to be selected.

All particles in the event, including the isolated tracks, were then clustered into jets using the JADE algorithm [11] with $y_{min} = 0.01$. For each isolated track the fraction of jet energy R was defined as the ratio of its momentum to the total momentum of the jet to which it belonged. Events in which this fraction was less than 0.75 for both of the isolated tracks were rejected.

The minimum value of this jet energy fraction, R_{min} , for both of the isolated tracks, together with the magnitude of the missing momentum, P_{miss} , was used for the final selection. Cases with two and one identified muons among the selected isolated tracks were considered separately because of the larger background in the latter case.

If two muons were identified the tagging variable y was defined as:

$$y = \frac{P^b(R_{min}) \cdot P^b(P_{miss})}{P^s(R_{min}) \cdot P^s(P_{miss})}, \quad (1)$$

where $P^{b,s}(R_{min})$, $P^{b,s}(P_{miss})$ are the probability density functions of R_{min} and P_{miss} , respectively, for background and signal events. Events were retained if $-\log_{10}(y) > -0.2$. In the case of only one reconstructed muon simpler cuts were applied: $R_{min} > 0.97$ and $P_{miss} < 30\text{ GeV}/c$.

Finally, in order to isolate the on-shell ZZ contribution, a kinematic fit (see section 5.2 in reference [1]) including four-momentum conservation was applied to the event. The event was selected as an on-shell ZZ candidate if the masses of both pairs of final state fermions lay within a window of $20\text{ GeV}/c^2$ of the nominal Z mass.

4.2 Results for the $\mu^+\mu^-q\bar{q}$ final state

The numbers of events observed before and after the mass selection are shown in table 3. For the case without mass cuts the signal is defined as all $\mu^+\mu^-q\bar{q}$ events; for the case with mass cuts the signal is the subset where both generated fermion pair masses lie within the mass window. Rather more events were observed in the data than were predicted by the simulation in this channel; three events were found in the high mass window at 183 GeV. We note that OPAL observed more events than predicted in this channel at 130-136 GeV[12]. A more detailed breakdown of the predicted background and a comparison of the number of events seen at various stages of the selection process is given in table 4. The predicted and observed distributions of the masses of the lepton and quark pairs for the $\mu^+\mu^-q\bar{q}$ and $e^+e^-q\bar{q}$ channels are shown in figure 1.

A second analysis based on sequential cuts which was optimized for the on-shell ZZ region found compatible results.

Energy(GeV)	All masses			$M_Z \pm 20 \text{ GeV}/c^2$		
	Data	Signal	Background	Data	Signal	Background
161	2	0.38 ± 0.04	0.09 ± 0.04	0	0 ± 0.01	0.006 ± 0.006
172	1	0.68 ± 0.05	0.09 ± 0.04	0	0 ± 0.01	0.006 ± 0.006
183	8	2.9 ± 0.2	0.43 ± 0.20	3	0.78 ± 0.13	0.03 ± 0.02

Table 3: The predicted numbers of signal and background events and the observed numbers of events in the $\mu^+\mu^-q\bar{q}$ channel at 161, 172 and 183 GeV centre-of-mass energies, with and without final mass cuts. The errors quoted are from simulation statistics.

selection	data	$\mu^+\mu^-q\bar{q}$	total back.	$q\bar{q}(\gamma)$	$\mu\nu q\bar{q}$	other back.	$\gamma\gamma \rightarrow$ hadr.
Hadronic	5092	10.8	4610 ± 22	3730	120	679	81
2 isolated tracks	209	3.9	175 ± 4	94	21	55	5
$\mu^+\mu^-$	50	3.6	42.5 ± 2	18.2	15.5	8.6	0.2
Fraction of jet energy	33	3.5	25.2 ± 1.5	4.5	15.2	5.5	0
final selection	8	2.9	0.43 ± 0.2	0.1	0	0.33	0
$M_{had} > 71.2 \text{ GeV}/c^2$	3	0.78	0.03 ± 0.02	0	0	0.03	0
$M_{\mu^+\mu^-} > 71.2 \text{ GeV}/c^2$							

Table 4: The numbers of events passing different steps of the selection procedure in the $\mu^+\mu^-q\bar{q}$ channel at $\sqrt{s} = 183 \text{ GeV}$.

4.3 $e^+e^-q\bar{q}$ final state.

Electrons passing through DELPHI are rather likely to interact with material before the electromagnetic calorimeters (the material in front of the HPC corresponds to $0.8X_0/\sin\theta$) and can also be produced in association with final state radiative photons. Both of these effects lead to tight clusters of charged and neutral particles in the detector, and criteria for selecting isolated electrons were devised to take this into account. Emphasis was placed on the reconstruction of narrow clusters around each electron candidate, so as to maximise the selection efficiency for events with both high e^+e^- and hadronic masses corresponding to on-shell ZZ production. In addition to the contribution from ZZ processes, processes such as single Z production $e^+e^- \rightarrow Z^0e^+e^-$ can produce events in the high mass region; both were treated as signal.

Each charged particle with momentum more than $5 \text{ GeV}/c$ was used as the seed for an electron cluster candidate. Any other particle (charged or neutral) with energy more than 2 GeV was included in the cluster if the resulting mass of the cluster remained below $0.4 \text{ GeV}/c^2$. The number of charged plus neutral particles in a cluster was limited to 3. Clusters with two charged particles of opposite sign were excluded to suppress backgrounds from photon conversions.

The charge of an electron cluster was defined as the charge of the seed particle. The direction was determined from the sum of momenta of the particles included in the cluster and the energy was taken to be the sum of the energies of the particles. For charged particles in the cluster the value used for the energy was the greater of the energy deposited in the electromagnetic calorimeter and the momentum measured by the tracking system.

The cluster was identified as a tight electron candidate if the energy deposited in the electromagnetic calorimeter (E_{EM}) exceeded 60% of the cluster energy or if $E_{EM} > 15$ GeV, the energy deposited in the first layer of the hadron calorimeter was less than 12 GeV and that beyond the first layer was less than 2.5 GeV.

In some cases the energy of the electron measured in the electromagnetic calorimeter was not sufficient for tight electron identification. This happened mainly because of insensitive zones present in the electromagnetic coverage. To increase the electron selection efficiency a loose identification condition was defined: the seed of an electron cluster candidate was required to be identified as a loose electron by the standard DELPHI identification package [4] and to have less than 7 GeV of energy deposited beyond the first layer of the hadron calorimeter. If the cluster did not point to an insensitive calorimeter region, the energy of the cluster seed was required to exceed 30 GeV.

Events considered in the analysis were required to have at least 6 charged tracks and a charged energy above $0.3 \sqrt{s}$. At least two identified electron clusters of opposite sign were required and at least one of them was required to be a tight electron candidate. The energy of each cluster was required to exceed 15 GeV. The energy of all charged particles not included in the cluster but within a cone of 5° around its direction was required to be below 4 GeV.

All particles not included in the electron clusters were clustered into jets using the JADE algorithm [11] with $y_{min} = 0.01$, and the transverse momentum of each electron candidate with respect to the nearest jet was computed. A strong suppression of background was obtained by demanding that the transverse momentum exceed 5 GeV/ c if the energy of the cluster seed was more than 20 GeV, 9 GeV/ c if this energy was more than 15 GeV and 15 GeV/ c if the energy of the cluster seed was less than 15 GeV. The stronger cuts on the transverse momentum with decreasing seed energy were necessary because of the increasing background arising from cluster seeds with small energies wrongly identified as electrons.

Events with one loose electron candidate have higher background contamination so additional cuts were applied to this subsample. It was found that this background comes mainly from WW events with one of the W bosons decaying into $e\nu$ and the other hadronically. To suppress this background the absolute value of the total reconstructed momentum of the event was required to be less than 50 GeV/ c . In addition, the transverse momentum of any cluster with loose electron identification was required to be more than 12 GeV/ c if the cluster pointed to an insensitive zone of electromagnetic calorimeter and more than 15 GeV/ c otherwise.

4.4 Results for the $e^+e^-q\bar{q}$ channel

The number of events found at each energy and the predicted numbers of signal and background events are shown in table 5, with and without the final mass cuts. More details of the background rejection and signal selection efficiencies at different steps of the analysis at 183 GeV are shown in table 6. The predicted and observed distributions of

the masses of the lepton and quark pairs for the $\mu^+\mu^-q\bar{q}$ and $e^+e^-q\bar{q}$ channels are shown in figure 1.

A second analysis based on sequential cuts which was optimized for the on-shell ZZ region found compatible results.

Energy(GeV)	All masses			$M_Z \pm 20\text{GeV}/c^2$		
	Data	Signal	Background	Data	Signal	Background
161	0	0.31 ± 0.03	0.13 ± 0.05	0	0.02 ± 0.02	0.006 ± 0.006
172	1	0.45 ± 0.04	0.13 ± 0.05	0	0.02 ± 0.02	0.006 ± 0.006
183	3	2.9 ± 0.2	0.56 ± 0.24	1	0.92 ± 0.12	0.03 ± 0.02

Table 5: The predicted numbers of signal and background events and the observed numbers of events in the $e^+e^-q\bar{q}$ channel at 161, 172 and 183 GeV centre-of-mass energies, with and without final mass cuts. The errors quoted are from simulation statistics.

selection	data	$e^+e^-q\bar{q}$	total back.	$q\bar{q}(\gamma)$	$e\nu q\bar{q}$	other back.	$\gamma\gamma \rightarrow$ hadr.
Hadronic	5092	16.2	4605 ± 22	3730	120	674	81
e identif.	993	10.8	1029 ± 11	820	56	136	17
e momenta	274	7.0	266 ± 5	210	24	24	7.7
Isolation	43	4.9	46.8 ± 3	26.1	10.6	7.1	3.0
$M_{e^+e^-} > 5 \text{ GeV}/c^2$	25	4.1	20.8 ± 2	8.2	7.5	3.5	1.6
p_t	3	2.6	1.43 ± 0.4	0.20	0.83	0.4	0.0
cuts for loose e	3	2.5	0.38 ± 0.1	0.05	0.13	0.20	0.0
$M_{e^+e^-} > 71.2 \text{ GeV}/c^2$							
$M_{had} > 71.2 \text{ GeV}/c^2$	1	0.92	0.03 ± 0.02	0.01	0.01	0.01	0.00

Table 6: The numbers of events passing different steps of the selection procedure in the $e^+e^-q\bar{q}$ channel at $\sqrt{s} = 183 \text{ GeV}$.

5 Four leptons

There are six possible four-lepton final states: $e^+e^-e^+e^-$, $e^+e^-\mu^+\mu^-$, $e^+e^-\tau^+\tau^-$, $\mu^+\mu^-\mu^+\mu^-$, $\mu^+\mu^-\tau^+\tau^-$ and $\tau^+\tau^-\tau^+\tau^-$. The event selection has been restricted to topologies with four charged tracks, implying that in the $e^+e^-\tau^+\tau^-$, $\mu^+\mu^-\tau^+\tau^-$ and $\tau^+\tau^-\tau^+\tau^-$ cases only one-prong decays of the τ were considered. The events were required to have exactly four charged tracks reconstructed in the TPC and VD, and to have their sum of charges equal to zero. The following selection criteria were applied:

- The total charged energy was required to be larger than $0.25 \sqrt{s}$.
- The rectangular region of the (p_t, M_{vis}) plane defined by $|\sum \vec{p}_t| < 0.05 \sqrt{s}$ and $M_{inv} < 0.2 \sqrt{s}$ was excluded to suppress background from two-photon events.

- At least two leptons (electrons or muons) had to be identified.
- The minimum invariant mass of any triplet $l^+l^-l^+$ was required to be greater than 2 GeV. This cut is to suppress the $\tau^+\tau^-$ background in a one-prong versus three-prong decay topology.
- The invariant mass of two oppositely charged particles which were not identified as electrons or muons was required to be larger than 2 GeV. This removed the background coming from $l^+l^-q\bar{q}$ production where the low Q^2 quark pair fragmented into $\pi^+\pi^-$ (mainly via $\rho(770)$).
- At least two particles, each with momentum greater than 3 GeV/c, should be isolated i.e. no other charged particle within 5° .
- At most 6 neutral particles were allowed in the event.
- γ -conversions in the detector material were rejected by searching for pairs of particles with opposite charge either identified as electrons or not identified as hadrons or muons. The rejection was done by requiring: i) the sum of impact parameters in $r\phi$ to the primary vertex to be less than 5 mm; ii) the invariant mass to be greater than 50 MeV/c² in case of at least two VD hits on the track and 100 MeV/c² otherwise.

The background was estimated using the following simulated samples:

- all possible four-fermion background processes,
- $e^+e^- \rightarrow q\bar{q}(\gamma)$,
- $e^+e^- \rightarrow l^+l^-(\gamma)$, $l = e, \mu, \tau$ and
- $\gamma\gamma \rightarrow hadrons, e^+e^-, \mu^+\mu^-, \tau^+\tau^-$.

The selection cuts suppressed the background to low levels. The main contribution comes from four-fermion production (mainly $l^+l^-q\bar{q}$) and from $l^+l^-(\gamma)$ interactions. The predicted numbers of events from signal and various background processes are shown in table 7, without imposition of any cut to select events in the ZZ region. The errors quoted are from simulation statistics.

5.1 Results for the four charged lepton channel

The predicted numbers of events are relatively large for $e^+e^-l^+l^-$ channels, less for $\mu^+\mu^-\mu^+\mu^-$ and $\mu^+\mu^-\tau^+\tau^-$ and lowest for the case of $\tau^+\tau^-\tau^+\tau^-$ where the cross-section is very low and the efficiency was reduced because we considered only one-prong τ decays. Table 8 shows the observed and predicted numbers of events at each centre-of-mass energy. The three events at 130-136 GeV were all $e^+e^-e^+e^-$ and were all found in the sample coming from the LEP run in 1997. The two events at 172 GeV were both $e^+e^-\mu^+\mu^-$ events. Out of three events found at 183 GeV, two were classified as being $e^+e^-\mu^+\mu^-$ and one as $e^+e^-\tau^+\tau^-$. One of these candidates is shown in figure 2.

None of the events had masses consistent with on-shell ZZ production. The predicted number of events in the mass window was 0.077 ± 0.007 signal plus 0 ± 0.141 background

Predicted numbers of $l^+l^-l^+l^-$ events				
Process	130-140 GeV	161 GeV	172 GeV	183 GeV
$e^+e^-e^+e^-$	0.44 ± 0.02	0.30 ± 0.02	0.31 ± 0.02	1.14 ± 0.06
$e^+e^-\mu^+\mu^-$	0.55 ± 0.03	0.36 ± 0.02	0.35 ± 0.02	1.79 ± 0.09
$e^+e^-\tau^+\tau^-$	0.116 ± 0.006	0.077 ± 0.004	0.064 ± 0.003	0.29 ± 0.02
$\mu^+\mu^-\mu^+\mu^-$	0.148 ± 0.007	0.078 ± 0.004	0.066 ± 0.003	0.27 ± 0.01
$\mu^+\mu^-\tau^+\tau^-$	0.072 ± 0.004	0.046 ± 0.002	0.039 ± 0.002	0.16 ± 0.01
$\tau^+\tau^-\tau^+\tau^-$	0.0043 ± 0.0002	0.0027 ± 0.0001	0.0020 ± 0.0001	0.012 ± 0.001
total $l^+l^-l^+l^-$	1.33 ± 0.07	0.87 ± 0.04	0.83 ± 0.04	3.68 ± 0.18

Predicted numbers of background events				
Process	130-140 GeV	161 GeV	172 GeV	183 GeV
four fermions	0.030 ± 0.015	0.035 ± 0.012	0.045 ± 0.09	0.064 ± 0.029
$q\bar{q}(\gamma)$	0 ± 0.025	0 ± 0.012	0 ± 0.011	0 ± 0.007
$l^+l^-(\gamma)$	0 ± 0.2	0 ± 0.14	0.06 ± 0.10	0.05 ± 0.10
$\gamma\gamma$	0 ± 0.1	0 ± 0.02	0 ± 0.02	0 ± 0.03
total background	0.03 ± 0.34	0.035 ± 0.18	0.11 ± 0.22	0.11 ± 0.17

Table 7: Predicted numbers of events for $l^+l^-l^+l^-$ channels and various background sources for the integrated luminosities collected at different centre-of-mass energies. No cut has been applied to select the ZZ mass region.

at 183 GeV, 0.0131 ± 0.001 signal plus 0 ± 0.141 background at 172 GeV and negligible at lower energies.

Taking all the data together there was reasonable agreement with predictions, with 3 $e^+e^-e^+e^-$, 4 $e^+e^-\mu^+\mu^-$ and 1 $e^+e^-\tau^+\tau^-$ events found compared with 2.2, 3.1 and 0.6 events predicted respectively. In all channels taken together 8 events were selected in the energy range 130-183 GeV while 6.7 were expected.

E_{cms} (GeV)	Observed Events	Predicted Signal	Predicted Background
130-140	3	1.33 ± 0.07	0.03 ± 0.34
161	0	0.87 ± 0.04	0.04 ± 0.18
172	2	0.83 ± 0.04	0.11 ± 0.22
183	3	3.68 ± 0.18	0.11 ± 0.17

Table 8: Number of events observed for all $l^+l^-l^+l^-$ channels at each centre-of-mass energy and the predicted numbers of signal and background events.

6 The four-jet channel

The fraction of on-shell ZZ events with both Z bosons decaying hadronically is expected to be close to 50 %. These events typically produce final states with four or more jets. At LEP-2 energies, two other processes can produce events with such topologies: WW production (with subsequent hadronic decays of both W bosons) and $Z\gamma$ production accompanied by gluon radiation (hereafter referred to as QCD events). Since the on-shell ZZ cross-section is two orders of magnitude smaller than the background, powerful background reduction techniques are required to isolate it. As W bosons decay to b quarks very rarely, looking for $b\bar{b}$ pairs among the produced jets using standard b -tagging algorithms[13] allowed us to reduce the background very efficiently. This analysis was therefore directed towards final states where one of the on-shell Z s decays into $b\bar{b}$.

6.1 Preselection

A preselection[14] was applied to eliminate radiative and non-hadronic final state events and to reduce the QCD background. It selected multi-hadronic events with at least 18 charged tracks, total energy above 60% \sqrt{s} , and total neutral energy below 50% \sqrt{s} . It was also required that no photon with more than 30 GeV be present. Four-jet events were selected by requiring that the sum of the normalised Fox-Wolfram moments of order two and four be less than 1.1, and that their thrust be less than 0.92. Finally the DURHAM algorithm[15] was applied, forcing a four-jet configuration, and the event was retained if each one of its jets contained at least one charged particle and had a mass greater than 1.5 GeV/ c^2 .

The preselection reduced the QCD contribution to an effective cross-section of 4.4 pb, while the efficiency for four-quark states is around 90%, corresponding to a predicted cross-section of 7.0 pb.

Using all the data collected by DELPHI at a mean energy of 182.7 GeV, corresponding to an integrated luminosity of 53.95 pb⁻¹, 601 events were preselected in the data to be compared with 619 expected (241 QCD, 360 *WW*, 18 *ZZ*).

6.2 Explicit reconstruction of dijets

The three possible configurations of jet pairings for each event were examined in turn, and one was selected using the corresponding b-tagging information and dijet masses, calculated both with and without a kinematic fit making use of the four constraints from energy and momentum conservation.

A configuration was rejected if either of the unfitted dijet masses was below 35 GeV/*c*²; it was also rejected if either of the fitted masses fell outside a 20 GeV/*c*² window around the nominal *Z* mass. Additionally, in order to select on-shell *ZZ* events preferentially, the unfitted dijet mass difference was required to be less than 50 GeV/*c*².

If an event contained no configuration satisfying these requirements it was rejected. If several configurations were selected, the dijet b-tagging information was used to select between them. If only one configuration survived a strong dijet b-tagging criterion, then it was selected. If several survived, then the configuration giving masses closest to the *Z* mass was chosen. If none survived, a looser b-tagging criterion was used and the process was repeated. The total reconstructed mass was then defined as the sum of the fitted dijet masses for the best configuration.

A total of 336 events satisfied these requirements in the data, while 342 were expected from the simulation (67, 266 and 8 respectively from the QCD, *WW*, and *ZZ* processes). Figure 3 shows the spectrum of the mass distribution after this reconstruction procedure for the data and simulated QCD, *WW* and *ZZ* events.

6.3 Global discriminating variable

Several variables which discriminate against the QCD background were considered in the construction of a global discriminating variable. These were based on event shapes and jet differences and the sum of the second and fourth order normalised Fox-Wolfram moments, the product of the smallest angle between any pair of jets multiplied by the minimum jet energy, and the Durham jet algorithm parameter corresponding to the transition from three to four jets were used as inputs. The most effective variable against the *WW* background was found to be the combined b-tagging probability[16] of the selected dijet pairing.

A likelihood function was constructed as the product of the normalised ratio of the *ZZ* to the QCD and *WW* background probabilities for each of the above variables. Figure 4 shows the distribution of this likelihood for all events with a dijet pairing compatible with the *ZZ* hypothesis.

A two-dimensional distribution was then constructed plotting the value of this likelihood versus the sum of reconstructed dijet masses for each event. Figure 5 shows the distributions for the data and for the simulation. *ZZ* candidates were expected to have both a high likelihood and a reconstructed sum of dijet masses close to twice the *Z* mass. A global discriminating variable was constructed by ordering the events according to the signal (*ZZ*) to background (QCD+*WW*) ratio estimated from this distribution using a

shifted histogram technique[17], opening a bin around each event rather than using a fixed binning.

6.4 Results for the four-jet channel

Figure 6 shows the distribution of the global discriminating variable. The selected number of events is a function of the signal to background ratio chosen: for example, for a signal to background ratio of one and above, 1.15 ± 0.12 , 0.41 ± 0.05 and 0.74 ± 0.12 events are expected from the simulation from respectively ZZ , QCD and WW processes, while a total of 3 events were found in the data.

The predicted and observed distributions for the global discriminating variable show good agreement. In order to quantify the contribution of the ZZ process, a Kolmogorov counting test[18] was applied including and excluding the ZZ events from the simulation. A confidence level of 8% was found without the ZZ , compared with 69% when ZZ was included. We take this to be weakly indicative of the presence of hadronic on-shell ZZ events in the data.

The best candidate found is shown in figure 7. One of the dijets had two secondary vertices and was tagged as a $b\bar{b}$ and the mass of the other dijet was consistent with the Z mass both before and after the kinematic fit.

7 Conclusions

We have searched for events produced by neutral-current processes such as ZZ and $Z\gamma^*$ in final states $e^+e^-q\bar{q}$, $\mu^+\mu^-q\bar{q}$, $l^+l^-l^+l^-$ and $q\bar{q}q\bar{q}$ using data samples collected by the DELPHI detector at centre-of-mass energies ranging from 130 to 183 GeV.

Twenty-six events were observed, in reasonable agreement with the standard model prediction of 15.5 ± 0.4 signal events with a background of 2.9 ± 0.6 events from other processes. Within a mass window of 20 GeV/ c^2 around the mass of the Z , seven events were observed, compared with a prediction of 3.0 ± 0.2 signal events and a background of 1.2 ± 0.2 events. The probability of seeing seven events from the background processes alone is below one per mille; we interpret this as evidence for on-shell ZZ production.

References

- [1] DELPHI collaboration, P. Abreu *et al.*, E. Phys. J. **C2** (1998) 581.
- [2] DELPHI collaboration, P. Abreu *et al.*, Phys. Lett. **B397** (1997) 158.
- [3] D. Fassouliotis *et al.*, DELPHI Note 97-100 CONF 91, submitted to Jerusalem conference.
- [4] DELPHI Collaboration, P. Abreu *et al.*, Nucl. Instr. and Meth. **A378** (1996) 57.
- [5] DELSIM *Reference Manual*, DELPHI note, DELPHI 87-97 PROG-100
- [6] F.A. Berends, R. Pittau, R. Kleiss, *Comp. Phys. Comm.* **85** (1995) 437-452.
- [7] T. Sjöstrand, *Comp. Phys. Comm.* **39** (1986) 347; T. Sjöstrand, PYTHIA 5.6 and JETSET 7.3, CERN-TH/6488-92.
- [8] Y. Kurihara, J. Fujimoto, T. Munehisa, Y. Shimizu, KEK CP-035, KEK 95-126 (1995).
- [9] S. Nova, A. Olshevski, and T. Todorov, *A Monte Carlo event generator for two photon physics*, DELPHI note 90-35 PROG 152.
- [10] F. A. Berends, P. H. Daverveldt, R. Kleiss, *Comp. Phys. Comm.* **40** (1986) 271-284, 285-307, 309-326
- [11] T. Sjöstrand, *Comp. Phys. Comm.* **28** (1983), 229.
- [12] OPAL collaboration, G. Alexander *et al.*, Phys. Lett. **B316** (1996) 315.
- [13] G. Borisov, C. Mariotti, DAPNIA/Spp Report 97-06 and INFN/ISS Report 97-03, *Performance of b-tagging in DELPHI at LEP2*.
- [14] DELPHI Collaboration, P. Abreu *et al.*, *Search for neutral Higgs bosons in e^+e^- collisions at $\sqrt{s} = 183$ GeV* DELPHI note 98-95 CONF 163 (submitted to ICHEP98 conference).
- [15] S. Catani, Yu.L. Dokshitzer, M. Olson, G. Turnock and B.R. Webber Phys. Lett. **B269** (1991) 432.
- [16] G. Borisov, DELPHI 97-94 PHYS 716, *Combined b-tagging*.
- [17] M. Rosenblatt *Remarks on some non-parametric estimates of a density function*. *Annals of Mathematical Statistics* **27** (1956), 832-835.
- [18] A. N. Kolmogorov, *Giron. Inst. Ital. Attuari*, **4**, 83-91 (1933)

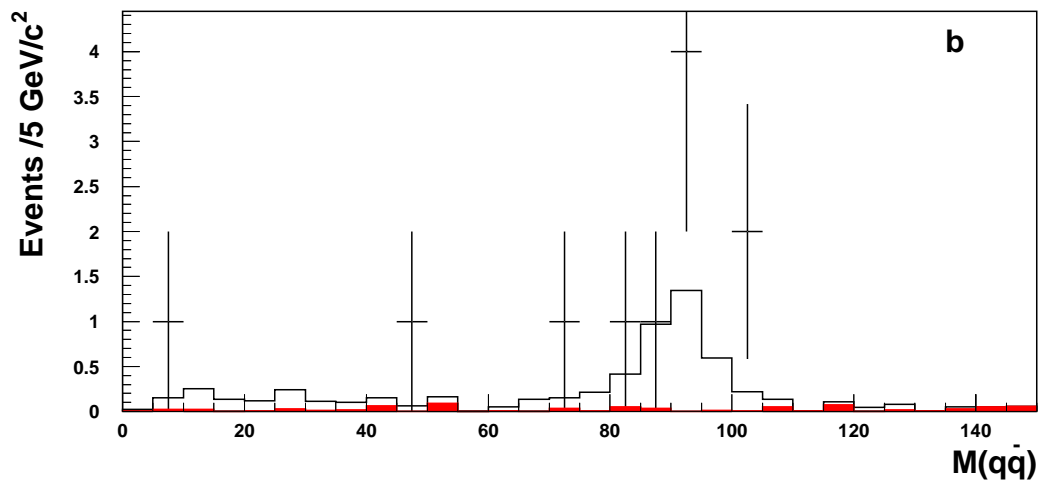
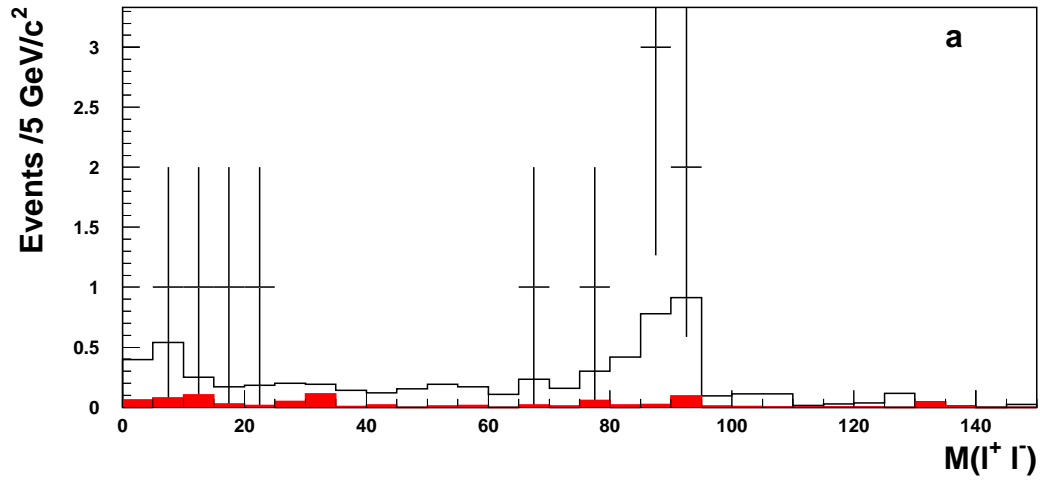



Figure 1: Masses of the lepton (a) and quark (b) pairs in $\mu^+\mu^-q\bar{q}$ and $e^+e^-q\bar{q}$ events at 183 GeV. The crosses are the data, the histogram is the prediction from simulation. The shaded region indicates the predicted contribution from background processes.

 DELPHI	Run: 80962	Evt: 2822					
	Beam: 91.6 GeV	Proc: 9-Dec-1997					
	DAS: 9-Nov-1997	Scan: 16-Jun-1998					
	16:37:43	DST					

	TD	TE	TS	TK	TV	ST	PA
Act	0	9	0	4	0	0	0
	(0 X 92 X	0 X	0 X	5 X	0 X	0 X	0)
Deact	0	0	0	0	0	0	0
	(0 X	0 X	0 X	0 X	0 X	0 X	0)

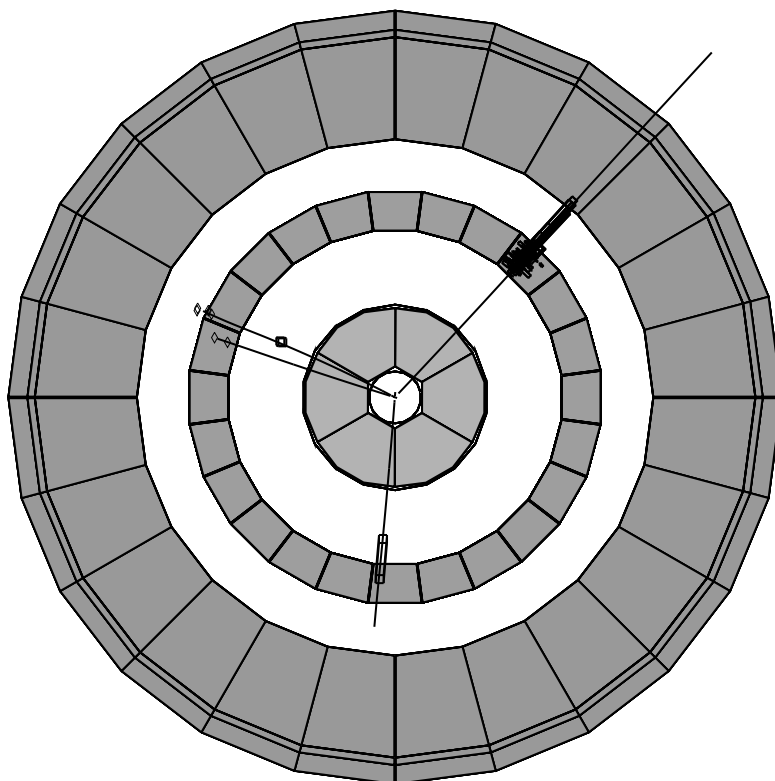


Figure 2: One of the $e^+e^-\mu^+\mu^-$ events selected at 183 GeV centre-of-mass energy. The two close tracks are muons reconstructed in the forward muon chambers. The two other tracks are electrons, one with energy deposited in HPC and the other in EMF.

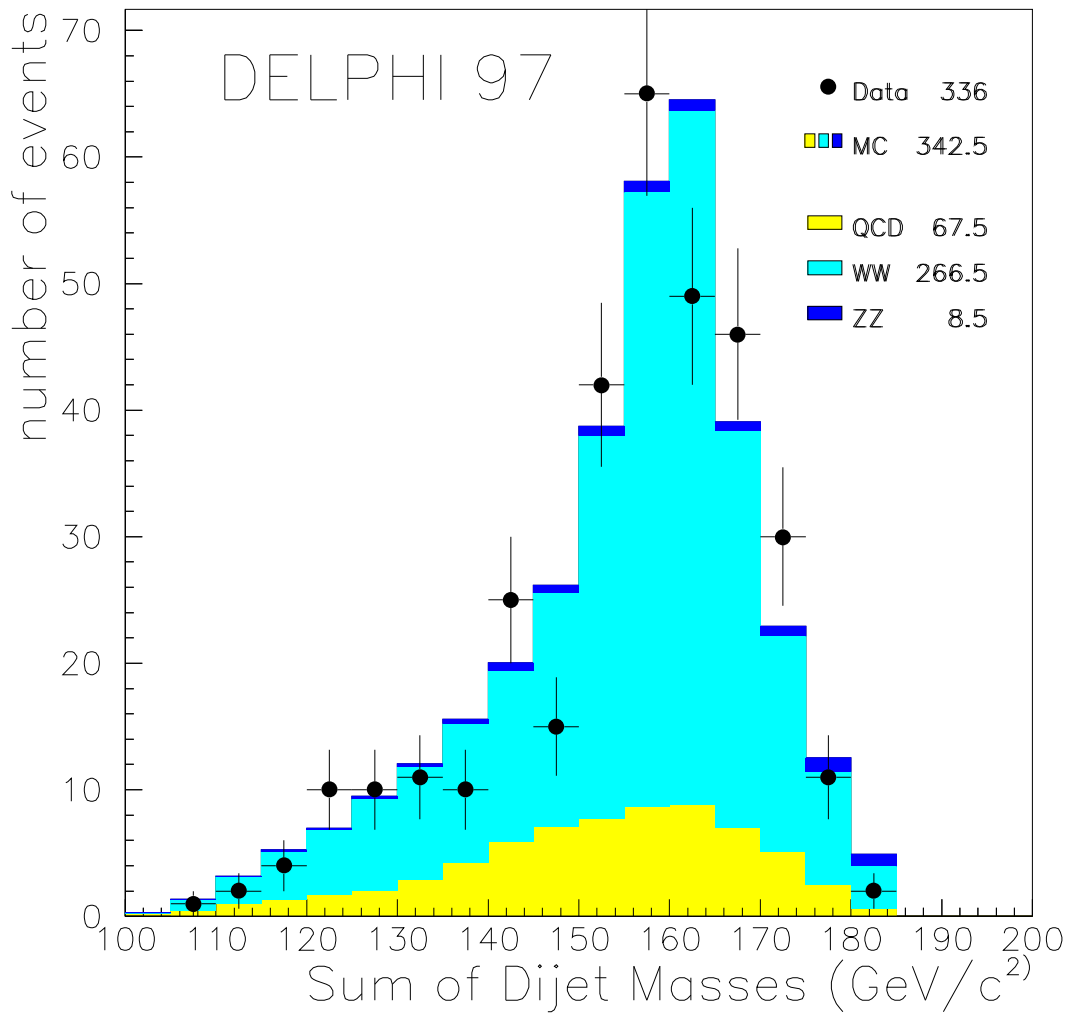


Figure 3: Distribution of the sum of the dijets masses satisfying a ZZ pairing in the four-jet channel at 183 GeV. The points with error bars are the data, the histogram is the prediction from simulation.

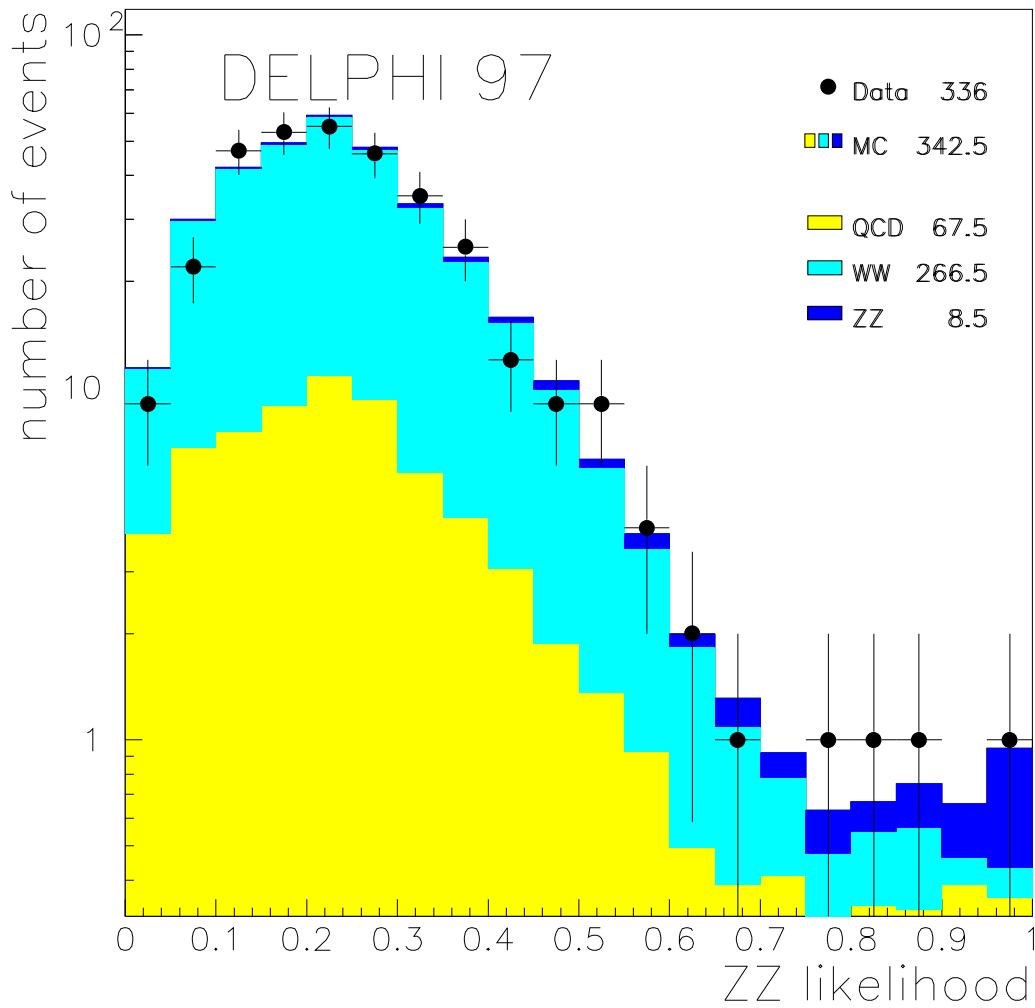


Figure 4: Distribution of the constructed likelihood for the expected signal (ZZ) and background (QCD and WW) in the four jet channel at 183 GeV. The points with error bars are the data, the histogram is the prediction from simulation.

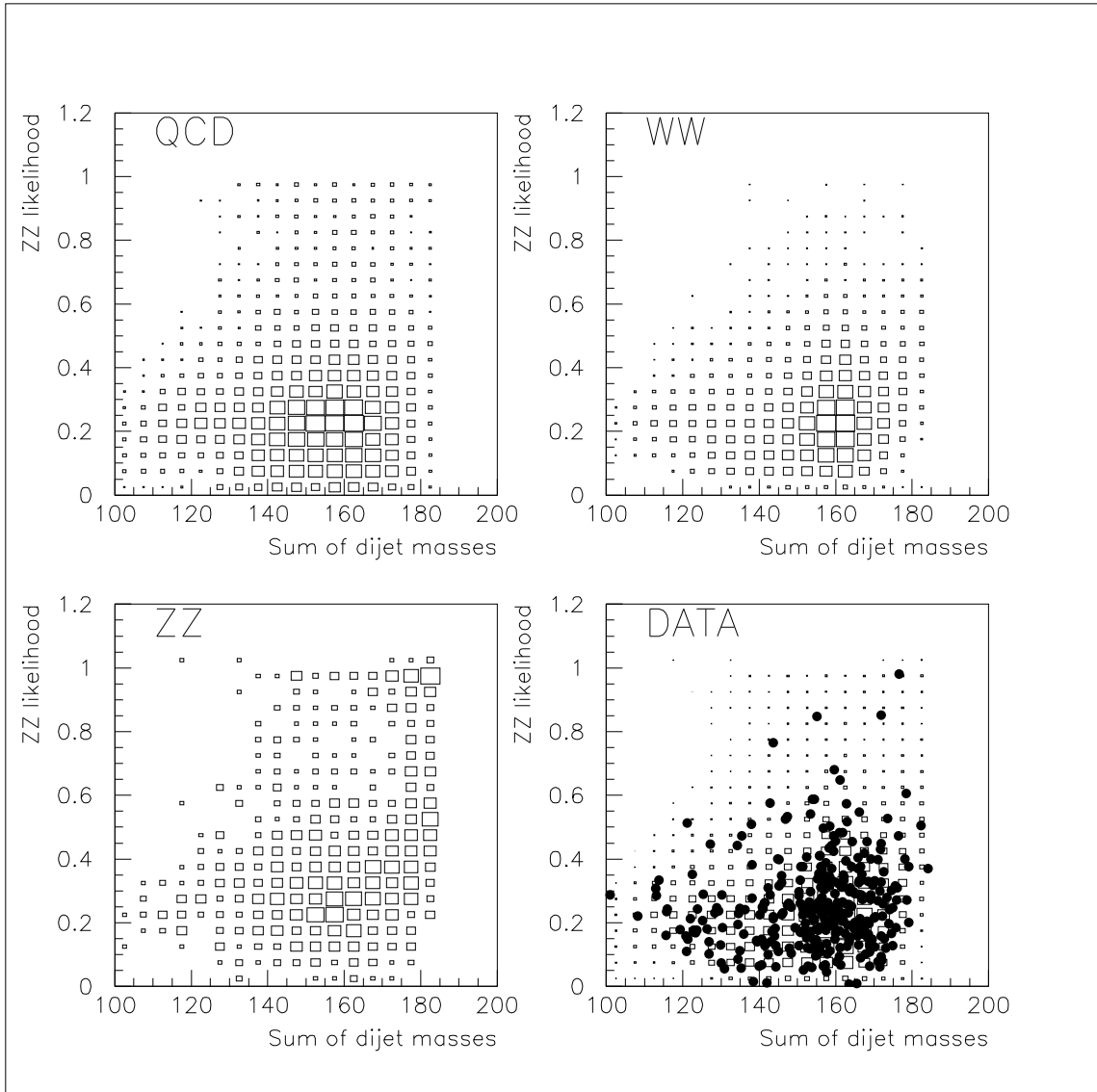


Figure 5: Two-dimensional distribution of the likelihood versus the sum of dijet masses for the background (top plots, left QCD , right WW), ZZ signal (left down), and real data (black dots, superimposed on total expectation from simulation) in the four jet channel at 183 GeV.

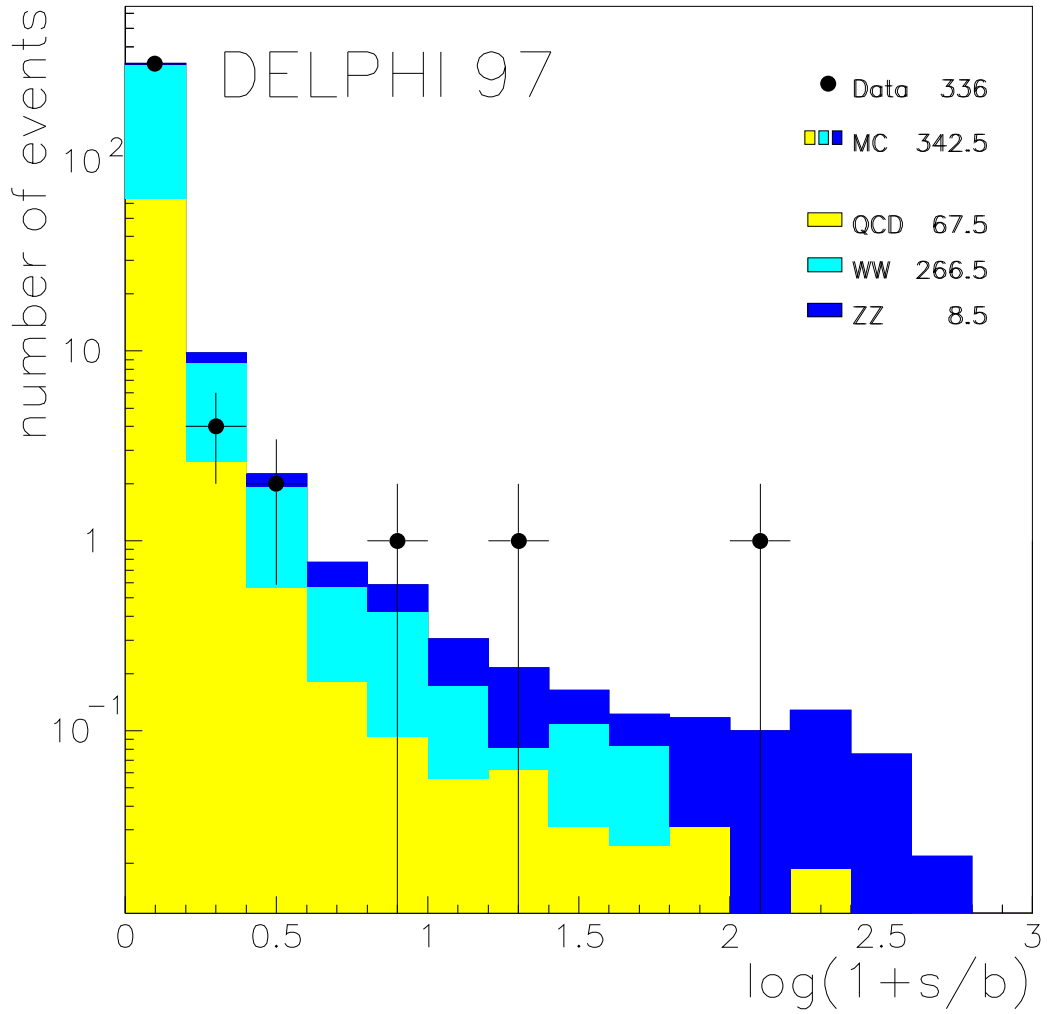


Figure 6: Distribution of the global discriminating variable for data (points with errors compared with QCD, WW and ZZ simulation for the four jet channel at 183 GeV. The signal to background ratio is expressed after a logarithmic transformation.

	DELPHI	Run: 77848	Evt: 4248	ID	YE	YB	YK	YV	YU	Yd				
	Beam: 91.0 GeV	Prod: 2-Dec-1997	Art	0	00	0	01	0	0	0				
	DAS: 15-Sep-1997	Scen: 16-Jan-1998	Descr	(0	X+20	X	0	Y	0	X	0	Y	0
	23:19:37	16n+DS1		0	0	0	0	0	0	0	0	0	0	

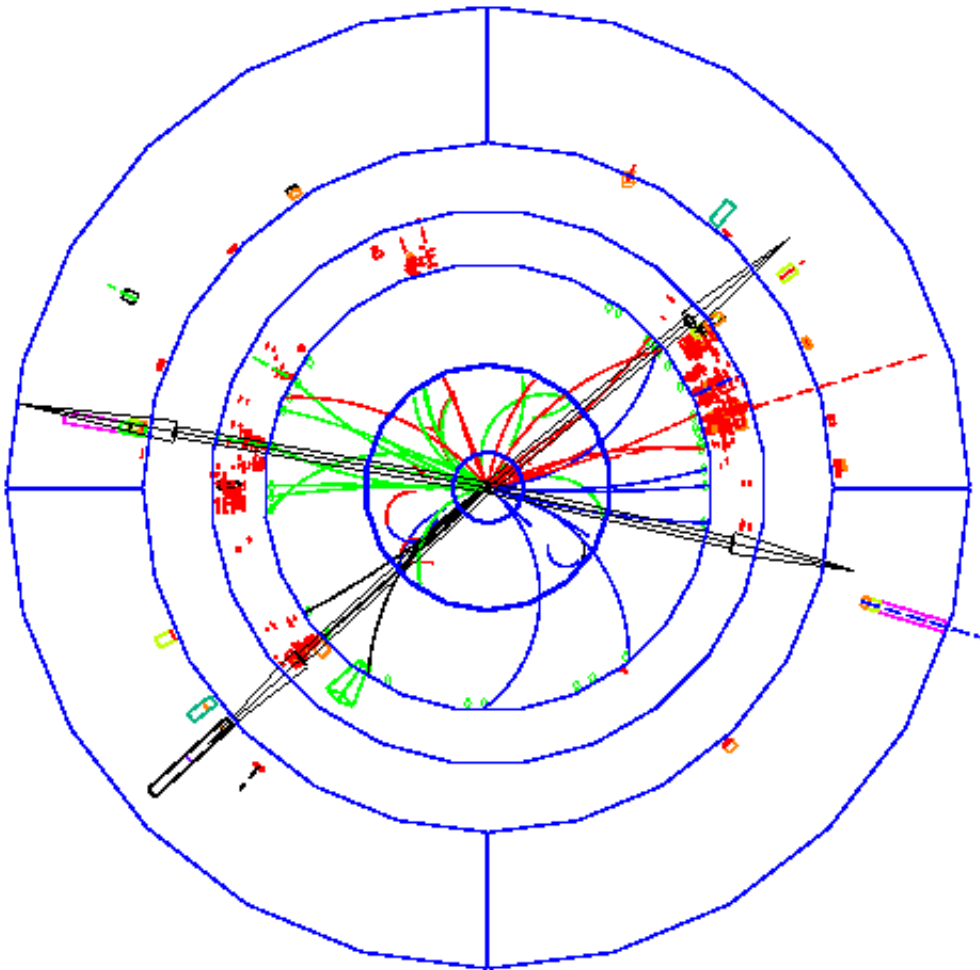


Figure 7: The ZZ four-jet candidate described in the text. Two jets were tagged as containing b quarks.